Geophysical Research Letters

RESEARCH LETTER
10.1029/2018GL077618

Coastal Sulfur Plumes off Peru During El Niño, La Niña, and Neutral Phases

T. Ohde[1]

[1]Laboratoire d'Etudes en Géophysique et Océanographie Spatiales (LEGOS), University of Toulouse, CNES, CNRS, IRD, UPS, Toulouse, France

Key Points:
- A MERIS-based identification algorithm is used to investigate surface sulfur plumes in the Peruvian coastal area
- The occurrence of coastal sulfur plumes is strongly coupled with the El Niño-Southern Oscillation
- During El Niños, the sulfur plumes disappear due to equatorial forced oxygenation, and La Niña's support the occurrence of sulfur plumes

Supporting Information:
- Supporting Information S1

Correspondence to:
T. Ohde,
thomas.ohde@legos.obs-mip.fr;
datusor@gmail.com

Citation:
Ohde, T. (2018). Coastal sulfur plumes off Peru during El Niño, La Niña, and neutral phases. *Geophysical Research Letters*, *45*, 7075–7083. https://doi.org/10.1029/2018GL077618

Received 2 MAR 2018
Accepted 4 JUL 2018
Accepted article online 11 JUL 2018
Published online 25 JUL 2018

Abstract For the first time, the impact of the El Niño-Southern Oscillation (ENSO) on the surface sulfur plumes off the Peruvian upwelling system has been studied. The investigations demonstrated a strong correlation between the ENSO and the sulfur plumes in the coastal areas of Callao and Pisco. During the El Niño phases, the sulfur plumes disappeared almost completely because of equatorial remotely forced oxygenation episodes. The La Niña events were associated with strong oxygen deficiency over the Peruvian shelf, supporting the formation of hydrogen sulfide and, consequently, the occurrence of sulfur plumes. This impact was smaller at Callao, because the La Niña phases in this coastal area were interrupted by weak oxygenation events. During the neutral phases, oxygen-poor waters were also present in the Peruvian shelf areas, promoting the large size of sulfur plumes. However, they were not forced by the remotely driven processes resulting from ENSO phenomena.

Plain Language Summary In the Peruvian coastal area, hydrogen sulfide outbreaks and their resulting coastal sulfur plumes influence the marine ecosystem and the fishing industry by their toxic properties. The relation between the sulfur plumes and the well-known El Niño and La Niña events was investigated. The sulfur plumes were detected in remotely sensed satellite data through their characteristic milky turquoise discoloration. The results demonstrated a strong correlation of the El Niño and La Niña events with the coastal sulfur plumes as well as their dependence on the oxygen supply in the Peruvian shelf area.

1. Introduction

In the coastal areas off the Namibian and Peruvian upwelling systems, hydrogen sulfide (H_2S) outbreaks influence the marine ecosystem owing to their toxic properties (Evans, 1967). Consequently, the abundance and availability of fish stocks can be reduced and human life can be negatively affected (Copenhagen, 1953). Sometimes, mass mortalities of fishes can be caused (Hamukuaya et al., 1998; Hart & Currie, 1960). For the local inhabitants, the strongest events were known as Callao painter (Brongersma-Sanders, 1948). They recognized them by the nasty smell of H_2S as well as by the paint darkening on boats and houses (Currie, 1953; Lavalle y Garcia, 1917). Most of these events were observed in the water regions off Callao and Pisco (Dugdale et al., 1977; Mears, 1943; Murphy, 1923). Other phenomena in the Peruvian region are the accumulation of diatomaceous mud at the sea bottom and the formation of an oxygen minimum zone (OMZ), both driven by the high primary production and the subsequent decomposition of the biomass (Kudrass, 2000; Karstensen et al., 2008; Schunck et al., 2013). The degradation of the organic matter in the sediment layers and in the water column promotes the formation of H_2S (Brüchert et al., 2003, 2006; Schunck et al., 2013). The flux of H_2S from the sediment to the bottom water layer is controlled by sulfide-oxidizing bacteria (Gutiérrez et al., 2008; Schulz et al., 1999). During the onset of upwelling favorable winds, the H_2S-enriched waters can be upwelled at the coastal regions (Ohde, 2009; Weeks et al., 2002, 2004). Such events manifest themselves by milky turquoise discolored surface waters (Ohde & Mohrholz, 2011; Weeks et al., 2004) caused by the formation of colloidal sulfur (S^O) by the oxidation of H_2S (Galán et al., 2014; Lavik et al., 2009; Schunck et al., 2013). Up to now, although these surface sulfur plumes have been investigated by a few studies in the Peruvian area (Mears, 1943; Schunck et al., 2013), most of them were only short reports (Burtt, 1852; Currie, 1953; Murphy, 1923).

The objective of the present paper is to investigate the relationships between coastal sulfur plumes off Peru and the El Niño-Southern Oscillation (ENSO). The ENSO describes basin-wide changes in air-sea interaction in the equatorial Pacific region with a timescale of about two to seven years (Glantz, 1996; Jiang et al., 1995; Setoh et al., 1999;

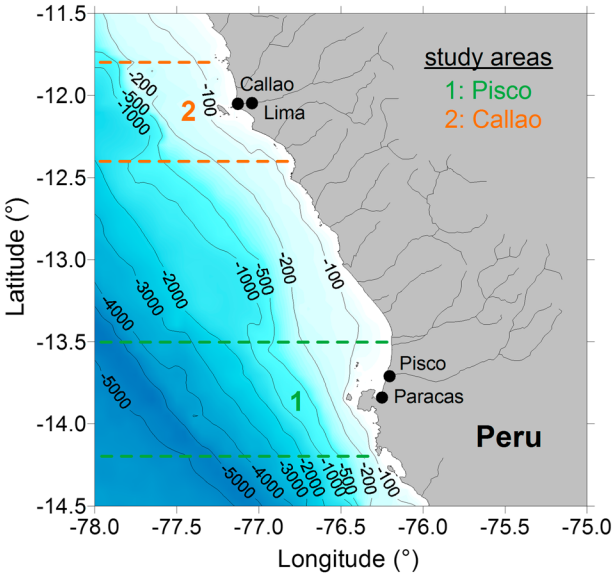

Figure 1. Study areas 1 (Pisco) and 2 (Callao) including the bathymetry (Amante & Eakins, 2009) and the main river system. The continental shelf is given as 200 m isobaths.

Torrence & Webster, 1999). Previous studies have shown teleconnections to extreme oceanic conditions in the Peruvian region, such as unusually warm water in the normally cold water coastal region (Enfield, 1989; Philander, 1990), changes in the coastal upwelling (Huyer et al., 1987; Ramage, 1975), and modifications in the abundance and composition of the phytoplankton (Carr et al., 2002; Correa-Ramirez et al., 2012; Thomas et al., 2001).

For investigating the influence of the ENSO on the Peruvian coastal sulfur plumes, first, such events are identified from ocean color satellites. As a result, time series of the sulfur plume size in two hot spots of Pisco and Callao from 2002 to 2012 are obtained. Second, the different ENSO phases are classified according to the most commonly used indices. As the remote forcing of the ENSO modulates the oceanic conditions in the Peruvian region, the hypothesis is that it also has a significant impact on the local temporal variability of sulfur plumes.

2. Data and Methods

2.1. Data

Daily Level-2 products of water-leaving reflectance with a spatial resolution of 1 km are used to identify the sulfur plumes in the coastal areas of Pisco (Figure 1, study area 1: 13.5°S–14.2°S) and Callao (Figure 1, study area 2: 11.8°S–12.4°S) in the time period from April 2002 to April 2012. The data were collected by the ocean color sensor MERIS (Medium Resolution Imaging Spectrometer) onboard the ENVISAT satellite of the European Space Agency (ESA). True color images of MERIS (spatial resolution: 1 km) and MODIS (Moderate Resolution Imaging Spectroradiometer; spatial resolution: 250 m) are compared with the detected sulfur plumes. The Japan Meteorological Agency Index (JMA: https://coaps.fsu.edu/), the Oceanic Niño Index (ONI: http://www.cpc.ncep.noaa.gov/), and the Multivariate ENSO Index (MEI: http://www.esrl.noaa.gov/) are the basis for the yearly classification system of the ENSO (see details in the supporting information). The JMA index is a five-month running mean of spatially averaged sea surface temperature anomalies over the tropical Pacific of 4°N–4°S and 90°W–150°W. The ONI is the standard of the National Oceanic and Atmospheric Administration (NOAA) and is defined as the three-month running mean of sea surface temperature anomalies in the Niño-3.4 region between 5°N–5°S and 120°W–170°W. The MEI is calculated from six combined variables over the tropical Pacific (Wolter, 1987; Wolter & Timlin, 1998).

2.2. Methods

The sulfur plumes are detected according to the method of Ohde et al. (2007), which was originally developed for Namibian waters. This method is adapted for the current study areas (Figure 1) by the analysis of the spectral characteristics of different Peruvian waters (onshore and offshore waters, algae blooms, river, and sulfur plumes). In 2009, a giant H_2S plume of about 440 km^3 was observed in the OMZ off Peru (Schunck et al., 2013). Strong correlations were found between this subsurface sulfidic plume and remotely sensed satellite sulfur plumes of turquoise discolored surface waters. Only the spectra of these validated sulfur plumes were used for the adaptation. The algorithm delivers the daily spatial extensions (size) of the sulfur plumes in the upper surface water layer. Sulfur concentrations lower than 631 nM cannot be detected with this algorithm (Ohde & Dadou, 2018). Note that the subsurface plumes can be overlooked by this method. This happens whenever the plumes remain in the deepwater layers. They can also be completely consumed by chemolithotrophic bacteria before they can reach the water surface (Lavik et al., 2009). Figure 2 illustrates an example for the identification of sulfur plumes. These plumes can be clearly seen as milky turquoise discolorations in the true color image of MERIS (Figure 2a). The comparison with Figure 2b demonstrates good conformity of the areas of turquoise discolorations with the identified sulfur pixels. River plume pixels can be well differentiated from sulfur pixels (e.g., Pisco river in Figures 2a and 2c). Much more details are visible in the MODIS scenes because of the higher spatial resolution (Figures 2c and 2d).

The daily size of sulfur plumes is determined in each of the 3,433 available MERIS scenes for the time period 2002–2012. From the daily values, a monthly integral of size is calculated. The error in the determination of

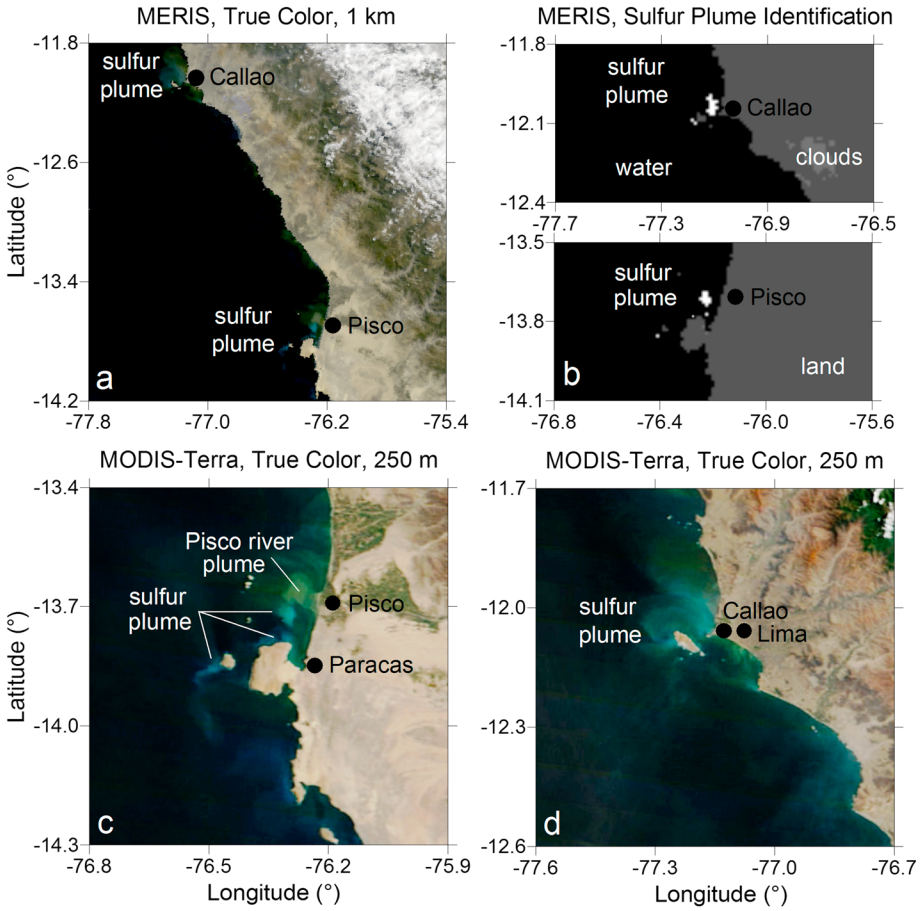

Figure 2. Example for the identification of sulfur plumes. (a) Sulfur plumes in a MERIS scene on 15 April 2009. (b) Detected sulfur pixels (white pixels). The sizes of the sulfur plumes are 23.1 and 29.9 km^2 in the study areas of Pisco and Callao, respectively. The dark gray and light gray pixels represent land and clouds, respectively. The black areas mark all water pixels, which are classified as no sulfur. (c) Sulfur and river plumes at Pisco in a MODIS-Terra scene on April 15, 2009. (d) Same figure as Figure 2c but in the Callao area.

the size is approximately 15% (Ohde & Dadou, 2018). The monthly integrals are compared with the ENSO indices to investigate the relation between sulfur plumes and the ENSO phenomena (Figures 3a and 3b). It is useful to divide the ENSO into three different phases: the El Niño (warm phase), La Niña (cold phase; often called El Viejo), and neutral phase (sometimes called normal phase). The ENSO year of October to the following September is identified as the El Niño if the JMA index is 0.5 °C or greater for six consecutive months (including October, November, and December). The year is categorized as La Niña if the JMA index is equal or smaller than −0.5 °C for six consecutive months (including October, November, and December). The El Niño and La Niña events based on ONI and MEI are further broken down into weak, moderate, and strong events. The classification of the ENSO years based on JMA, ONI, and MEI, which is given in Table 1, is described in the supporting information.

The JMA index defines three El Niño events, two La Niña events, and six neutral phases in the time period 2001–2012. To investigate the temporal variability of sulfur plumes in these three ENSO phases, the monthly values of the sulfur plume size are separately averaged over each phase (Figures 3c and 3d). As shown in Table 1, the JMA phases are only slightly different from the classifications based on ONI and MEI. Differences are mainly observed for some neutral phases, which are classified as the warm or cold phases, but mostly with weak intensities. The reason is the higher sensibility of the ONI and MEI compared to the JMA index (e.g., Hanley et al., 2003). Using the ONI and MEI, the El Niño JMA events of 2002–2003, 2006–2007, and 2009–2010 are classified as moderate, weak to moderate, and moderate warm phases, respectively. The La Niña JMA events of 2007–2008 and 2010–2011 are categorized as moderate to strong

Table 1
Classification of the ENSO Years Into Warm, Cold, and Neutral Phases Including Weak, Moderate, and Strong

ENSO-Year	JMA	ONI	MEI
2001-2002	neutral	neutral	neutral
2002-2003	warm	warm (moderate)	warm (moderate)
2003-2004	neutral	neutral	neutral
2004-2005	neutral	warm (weak)	neutral
2005-2006	neutral	cold (weak)	neutral
2006-2007	warm	warm (weak)	warm (moderate)
2007-2008	cold	cold (strong)	cold (moderate)
2008-2009	neutral	cold (weak)	cold (weak)
2009-2010	warm	warm (moderate)	warm (moderate)
2010-2011	cold	cold (strong)	cold (strong)
2011-2012	neutral	cold (moderate)	cold (weak)

Note. The classification is explained in the supporting information. An ENSO year is defined from October to the following September.

and strong, respectively. Furthermore, the statistical method of linear regression analysis is used to investigate the relations between the sulfur plumes and ENSO phases (Figures 4a–4f). For this purpose, the monthly values of the sulfur plume size and the different ENSO indices are separately averaged over each phase from October to April (see details in the supporting information). The full ENSO year from October to September is not used, because the months from May to September are often located within the transition phases of two different ENSO periods.

3. Results

Figure 3a presents the temporal variability of the sulfur plumes for the period from April 2002 to April 2012. Nearly no sulfur plumes are observed in the study areas during 2002–2003, 2006–2007, and 2009–2010. Their sizes are slightly increased at the beginning of 2004, 2007, and 2012. However, the largest sizes are found during 2004–2005, 2005–2006, 2007–2008, 2008–2009, and 2010–2011. The monthly sulfur plume size is often much higher in the Pisco area compared to that in the Callao area.

The JMA index, ONI, and MEI are given in Figure 3b. Up to now, there is no uniform view within the scientific community regarding which index is the best for the definition of ENSO years (e.g., Hanley et al., 2003). In Figure 3b, the JMA index is used for the determination of the main phases and strengths of ENSO, because this index is very robust (Hanley et al., 2003; Trenberth, 1997). The ONI and MEI are included to determine the timing and duration of these events. A strong correlation between the time series of the ENSO and the sulfur plumes is evident. During the El Niño phases (Table 1; JMA: 2002–2003, 2006–2007, and 2009–2010), hardly any sulfur plume is observed in the surface waters. However, the sulfur plume sizes are usually much larger during the neutral phases (Table 1; JMA: 2004–2005, 2005–2006, and 2008–2009) with the exceptions of 2003–2004 and 2011–2012. During the La Niña phases (Table 1; JMA: 2007–2008 and 2010–2011), the sulfur plume sizes in the coastal area of Callao are much smaller than in the neutral phases. However, the sizes at Pisco are in the same range or even larger than those in the neutral phases.

The temporal variability of sulfur plumes in the three ENSO phases is compared in the two study areas in Figures 3c and 3d. During the El Niño phase, the sulfur plumes are nearly vanished from October to April and from June to September in both study areas. Few sulfur plumes are observed in May. In the neutral phase, the sulfur plume sizes are very low from October to November and from June to September. Between these periods two maxima are observed. In the coastal areas of Pisco and Callao, the first maximum is in December. The second maximum in the Callao area is in March, two months earlier than that at Pisco. During the La Niña phase, the sulfur plume sizes at Pisco are normally smaller than during the neutral phase without considering October and the exceptional months of April and May. There are three maxima, located

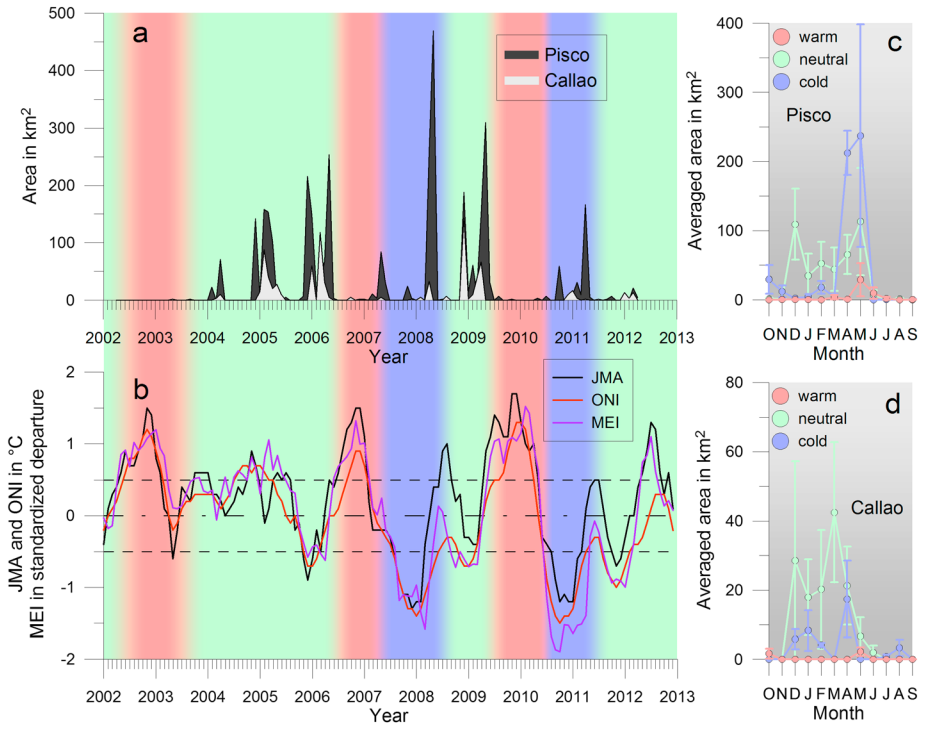

Figure 3. Comparison of sulfur plume sizes with the ENSO phases. (a) The sulfur plume sizes at Pisco (black curve) and Callao (gray curve) are given. (b) The ENSO indices are superimposed. The three phases, namely, the El Niño (warm phase, red stripes), La Niña (cold phase, blue stripes), and neutral phase (normal phase, green stripes), are classified according to the robust JMA index. The dashed lines represent −0.5, 0, and 0.5 °C. (c) Averaged temporal variability of sulfur plumes including the standard deviations in the Pisco area during the different ENSO phases. (d) Same figure as Figure 3c, however for Callao.

in October, February, and May. In contrast, the sulfur plume sizes at Callao are always smaller than in the neutral phase without considering the months of July and August. Again, there are three maxima, located in August, January, and April, which are one to two months earlier than the maxima at Pisco. Another difference between the study areas is the generally higher sulfur plume size in the Pisco area.

The sulfur plume size and the ENSO indices, which are averaged over the monthly values of the main ENSO periods from October to April, are plotted in Figures 4a–4f. The points of moderate to strong warm and cold phases generate clusters if they are classified according to the different ENSO phases given in Table 1. Most of the other points of the neutral phases as well as of the weak warm and cold phases are strongly scattered in the *x*-*y* plane nearly within the limits of 0.5 and −0.5 °C. They are ranged from low to high sulfur plume sizes. Some of them are shifted to the highest observed averaged sizes. Significant linear relations are determined by a correlation analysis for the points of warm and cold phases, which were moderate and strong. There is no significant correlation for the ONI at Pisco. The Pearson's correlation coefficients vary between −0.97 and −0.98, and the confidence limits are 99% (without the ONI at Pisco).

4. Discussion

During the observation period, a close relation between sulfur plumes and the moderate to strong warm or cold phases is evident through the correlation analysis (Figures 4a–4f).

The almost complete disappearance of the sulfur plumes during the El Niño phases (Figures 3c and 3d) can be explained mainly by equatorial remotely forced oxygenation episodes. The poleward propagation of trapped coastal waves forced by equatorial Kelvin waves often increases the oxygen level on the continental shelf (Gutiérrez et al., 2008). These waves occur more frequently during the warm El Niño phases (Camayo & Campos, 2006; Pizarro et al., 2001). Extreme oxygenation events originating from these wave-induced

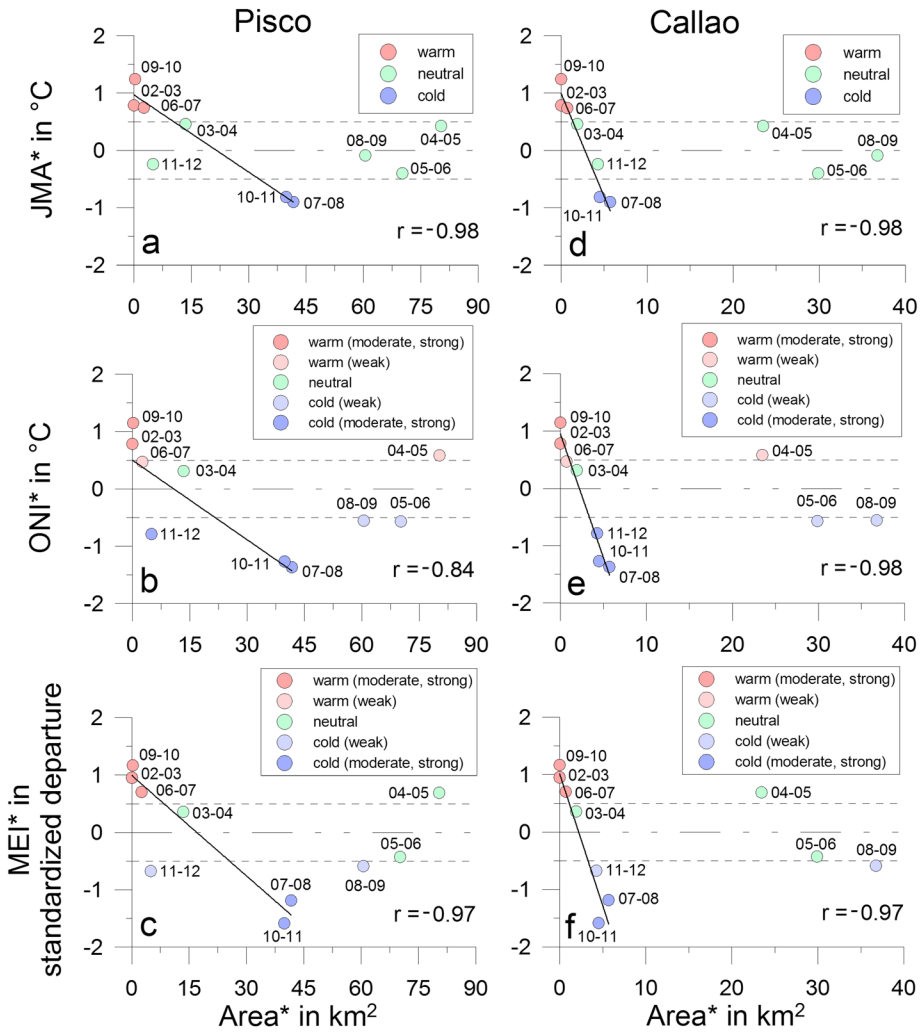

Figure 4. Relation between sulfur plumes and ENSO phases. The Pearson correlation coefficients are given. The values beside the colored points correspond to the different ENSO periods. (a–c) Correlation analysis for the Pisco area. (d–f) Correlation analysis for Callao.

conditions were evidenced in the bottom water column off the coast of Callao during 2002–2003, 2006–2007, and 2009–2010 (Graco et al., 2017). They occurred at the same time as the disappearance of the surface sulfur plumes. These events were generally accompanied by a deepening of the oxycline (Hamersley et al., 2007) and a reduction in the OMZ volume (Gutiérrez et al., 2008; Helly & Levin, 2004; Sánchez et al., 1999). The oxygenation episodes can reduce the H_2S formation that commonly occurs in anoxic marine sediments through microbial sulfate reduction (Jørgensen, 1982; Lein, 1984), can impact the flux of H_2S from the upper sediment to the bottom water layer usually controlled by sulfide-oxidizing bacteria (Ferdelman et al., 1997; Schulz et al., 1999), and can provide the removal of the H_2S-enriched water by biological (Galán et al., 2014; Lavik et al., 2009; Schunck et al., 2013) and possibly chemical oxidation processes (Gutiérrez et al., 2008). The disappearance of the sulfur plumes is also intensified by the absence of upwelling during the El Niño phases.

The La Niña phases are associated with the shoaling of the oxycline and a water column dominated by suboxic conditions (Hamersley et al., 2007). During these phases, strong oxygen deficiency occurs over the Peruvian shelf, and surface sediments tend to be anoxic, promoting microbial sulfate reduction and formation of H_2S (Tyson & Pearson, 1991). Such remotely forced anoxic conditions were observed during the moderate to strong La Niña events of 2007–2008 and 2010–2011 (Graco et al., 2017), resulting in larger sulfur plume sizes (Figures 3a–3d). The smaller sizes at Callao may be because of the weak oxygenation

events in 2008 and 2011 (Graco et al., 2017), probably driven by the local effect of cross-shore ventilation. These short events reduce the probability of the formation of H_2S-enriched bottom water.

During the neutral phases, oxygen-depleted subsurface water can also be observed (Tyson & Pearson, 1991). The oxygen-poor waters can intercept the Peruvian shelf areas, promoting suboxic and even anoxic conditions in the bottom water layer, which would support the formation of H_2S and the occurrence of surface sulfur plumes. Such conditions were found in the Callao area during the neutral phases in 2003–2006, 2008–2009, and 2011–2012 (Graco et al., 2017; Gutiérrez et al., 2008). The giant subsurface sulfidic plume observed in January 2009 (Schunck et al., 2013) was most likely the source of the satellite-detected sulfur plumes at the beginning of that year (Figure 3a). The small sulfur plume sizes in the neutral phase of 2003–2004 were probably caused by the slow transition of biogeochemical processes from oxic to anoxic conditions. The sizes were particularly large after the La Niña events, except for 2011–2012. The reason was the lack of MERIS data. However, MODIS data after April 2012 indicated an increase in sulfur events. The sulfur plumes in the neutral phases are normally not forced by remotely driven processes arising from ENSO events, because no correlation exists with the ENSO indices (Figures 4a–4f).

5. Conclusions

The hypothesis given in the introduction was confirmed. It was demonstrated that the ENSO phenomena significantly influence the sulfur plumes in the surface water in the coastal areas of Callao and Pisco. During the El Niño events of 2002–2003, 2006–2007, and 2009–2010, the sulfur plumes disappeared almost completely because of equatorial remotely forced oxygenation episodes. The La Niña events of 2007–2008 and 2010–2011 were associated with strong oxygen deficiency over the Peruvian shelf, supporting the occurrence of sulfur plumes. During the neutral phases of 2003–2006, 2008–2009, and 2011–2012, the anoxic conditions in the bottom water layers also promoted the large size of sulfur plumes. However, this was not forced by the remotely driven processes of ENSO phenomena.

6. Data Availability

The reflectance data were obtained from the ESA (https://merisrr-merci-ds.eo.esa.int/). The images of MODIS were downloaded from the Rapid Response System (https://earthdata.nasa.gov/). The ENSO indices were available through the Center for Ocean-Atmospheric Prediction Studies (https://coaps.fsu.edu/), the Climate Prediction Center (http://www.cpc.ncep.noaa.gov/), and the Earth System Research Laboratory (http://www.esrl.noaa.gov/).

Acknowledgments
This project has received funding from the Marie Skłodowska-Curie Actions grant agreement 706426. I thank the host institute OMP/LEGOS (Observatoire Midi-Pyrénées/ Laboratoire d'Etudes en Géophysique et Océanographie Spatiales). I thank the anonymous reviewers. The MERIS data were provided by the ESA. I acknowledge the use of MODIS imagery from the NASA/GSFC/Earth science data system. All data sets are available at the given websites and the supporting information.

References

Amante, C., & Eakins, B. W. (2009). ETOPO1 1 arc-minute global relief model: Procedures, data sources and analysis. *NOAA Technical Memorandum NESDIS NGDC-24*. National Geophysical Data Center, NOAA. https://doi.org/10.7289/V5C8276M

Brongersma-Sanders, M. (1948). The importance of upwelling water to vertebrate paleontology and oil geology. *Verhandelingen der Koninklyke Nederlandsche. Tweede Sectie, Deel*, *XLV*(4), 112.

Brüchert, V., Currie, B., Peard, K. R., Lass, U., Endler, R., Dübecke, A., et al. (2006). Biogeochemical and physical control on shelf anoxia and water column hydrogen sulphide in the Benguela coastal upwelling system off Namibia. In L. Neretin, et al. (Eds.), *Past and present water column anoxia, NATO Science Series. IV. Earth and Environmental Sciences* (pp. 161–193). Netherlands: Kluwer Springer.

Brüchert, V., Jørgensen, B. B., Neumann, K., Riechmann, D., Schloesser, M., & Schulz, H. (2003). Regulation of bacterial sulfate reduction and hydrogen sulphide fluxes in the central Namibian coastal upwelling zone. *Geochimica et Cosmochimica Acta*, *67*(23), 4505–4518. https://doi.org/10.1016/S0016-7037(03)00275-8

Burtt, J. L. (1852). On fish destroyed by sulphuretted hydrogen in the Bay of Callao. *American Journal of Science*, *2*(13), 433–434.

Camayo, R., & Campos, E. J. D. (2006). Application of wavelet transform in the study of coastal trapped waves off the west coast of South America. *Geophysical Research Letters*, *33*, L22601. https://doi.org/10.1029/2006GL026395

Carr, M., Strub, P., Thomas, A., & Blanco, J. (2002). Evolution of 1996–1999 La Niña and El Niño conditions off the western coast of South America: A remote sensing perspective. *Journal of Geophysical Research*, *107*(C12), 3226. https://doi.org/10.1029/2001JC001183

Copenhagen, W. J. (1953). The periodic mortality of the fish in the Walvis Bay region – A phenomenon within the Benguela Current. *Investigational Report Division of Fisheries-Union of south Africa*, *14*, 1–35.

Correa-Ramirez, M. A., Hormazabal, S. E., & Morales, C. E. (2012). Spatial patterns of annual and interannual surface chlorophyll-a variability in the Peru–Chile Current System. *Progress in Oceanography*, *92–95*, 8–17.

Currie, R. (1953). The Callao Painter. *Weather*, *8*(10), 308–311.

Dugdale, R. C., Goering, J. J., Barber, R. T., Smith, R. L., & Packard, T. T. (1977). Denitrification and hydrogen sulfide in the Peru upwelling region during 1976. *Deep-Sea Research*, *24*(6), 601–608. https://doi.org/10.1016/0146-6291(77)90530-6

Enfield, D. B. (1989). El Niño, past and present. *Reviews of Geophysics*, *27*(1), 159–187. https://doi.org/10.1029/RG027i001p00159

Evans, C. L. (1967). The toxicity of hydrogen sulphide and other sulphides. *Quarterly Journal of Experimental Psychology*, *52*, 231–248.

Ferdelman, T. G., Lee, C., Pantoja, S., Harder, J., Bebout, B. M., & Fossing, H. (1997). Sulfate reduction and methanogenesis in a Thioploca-dominated sediment off the coast of Chile. *Geochimica et Cosmochimica Acta*, *61*(15), 3065–3079. https://doi.org/10.1016/S0016-7037(97)00158-0

Galán, A., Faúndez, J., Thamdrup, B., Santibáñez, J. F., & Farías, L. (2014). Temporal dynamics of nitrogen loss in the coastal upwelling ecosystem off central Chile: Evidence of autotrophic denitrification through sulfide oxidation. *Limnology and Oceanography*, *59*(6), 1865–1878. https://doi.org/10.4319/lo.2014.59.6.1865

Glantz, M. H. (1996). *Currents of Change: El Niño's Impact on Climate and Society* (p. 194). Cambridge: Cambridge University Press.

Graco, M. I., Purca, S., Dewitte, B., Castro, C. G., Morón, O., Ledesma, J., et al. (2017). The OMZ and nutrient features as a signature of inter-annual and low-frequency variability in the Peruvian upwelling system. *Biogeosciences*, *14*(20), 4601–4617. https://doi.org/10.5194/bg-14-4601-2017

Gutiérrez, D., Enríquez, E., Purca, S., Quipúzcoa, L., Marquina, R., Flores, G., & Graco, M. (2008). Oxygenation episodes on the continental shelf of central Peru: Remote forcing and benthic ecosystem response. *Progress in Oceanography*, *79*(2–4), 177–189. https://doi.org/10.1016/j.pocean.2008.10.025

Hamersley, M. R., Lavik, G., Woebken, D., Rattray, J. E., Lam, P., Hopmans, E. C., et al. (2007). Anaerobic ammonium oxidation in the Peruvian oxygen minimum zone. *Limnology and Oceanography*, *52*(3), 923–933. https://doi.org/10.4319/lo.2007.52.3.0923

Hamukuaya, H., O'Toole, M. J., & Woodhead, P. M. J. (1998). Observations of severe hypoxia and offshore displacement of Cape hake over the Namibian shelf in 1994. *South African Journal of Marine Science*, *19*(1), 57–59. https://doi.org/10.2989/025776198784126809

Hanley, D. E., Bourassa, M. A., O'Brien, J. J., Smith, S. R., & Spade, E. R. (2003). A quantitative evaluation of ENSO indices. *Journal of Climate*, *16*(8), 1249–1258. https://doi.org/10.1175/1520-0442(2003)16<1249:AQEOEI>2.0.CO;2

Hart, T. J., & Currie, R. I. (1960). The Benguela Current. In *Discovery Report 31* (pp. 123–298). Cambridge: Cambridge University Press.

Helly, J. J., & Levin, L. A. (2004). Global distribution of naturally occurring marine hypoxia on continental margins. *Deep-Sea Research Part I*, *51*(9), 1159–1168. https://doi.org/10.1016/j.dsr.2004.03.009

Huyer, A., Smith, R. L., & Paluszkiewicz, T. (1987). Coastal upwelling off Peru during normal and El Niño times, 1981–1984. *Journal of Geophysical Research*, *92*(C13), 14,297–14,307. https://doi.org/10.1029/JC092iC13p14297

Jiang, N., Neelin, J. D., & Ghil, M. (1995). Quasi quadriennal and quasi-biennal variaility in the equatorial pacific. *Climate Dynamics*, *12*(2), 101–112. https://doi.org/10.1007/BF00223723

Jørgensen, B. B. (1982). Ecology of the bacteria of the Sulphur cycle with special reference to anoxic-oxic interface environments. *Philosophical Transactions of the Royal Society of London*, *B298*(1093), 543–561.

Karstensen, J., Stramma, L., & Visbeck, M. (2008). Oxygen minimum zones in the eastern tropical Atlantic and Pacific oceans. *Progress in Oceanography*, *77*(4), 331–350. https://doi.org/10.1016/j.pocean.2007.05.009

Kudrass, H. (2000). Cruise report Sonne-147–Peru upwelling, BGR Rep.0120607–11672/00, *Bundesanst. für Geowiss. und Rohst*., Hannover, *Germany*.

Lavalle y Garcia, J. A. (1917). Informe preliminar sobre la causa de la mortalidad anormal de las aves ocurrida en el mes de marzo del presente ano. *Memoria Compania Administradova del Guano*, *8*, 61–88.

Lavik, G., Stührmann, T., Brüchert, V., van der Plas, A., Mohrholz, V., Lam, P., et al. (2009). Detoxification of sulphidic African shelf waters by blooming chemolithotrophs. *Nature*, *457*(7229), 581–584. https://doi.org/10.1038/nature07588

Lein, A. Y. (1984). Anaerobic consumption of organic matter in modern marine sediments. *Nature*, *312*(5990), 148–150. https://doi.org/10.1038/312148a0

Mears, E. G. (1943). The Callao Painter. *Scientific Monthly*, *57*, 331–336.

Murphy, R. C. (1923). The oceanography of the Peruvian littoral with reference to the abundance and distribution of marine life. *Geographical Review*, *13*(1), 64–85. https://doi.org/10.2307/208202

Ohde, T. (2009). Investigation of hydrogen sulphide eruptions along the Namibian coastline using different remote sensing systems. *Open Geosciences*, *1*(3), 340–346.

Ohde, T., & Dadou, I. (2018). Seasonal and annual variability of coastal Sulphur plumes in the northern Benguela upwelling system. *PLoS One*, *13*(2), e0192140. https://doi.org/10.1371/journal.pone.0192140

Ohde, T., & Mohrholz, V. (2011). Interannual variability of sulphur plumes off the Namibian coast. *International Journal of Remote Sensing*, *32*(24), 9327–9342. https://doi.org/10.1080/01431161.2011.554455

Ohde, T., Siegel, H., Reißmann, J., & Gerth, M. (2007). Identification and investigation of sulphur plumes along the Namibian coast using the MERIS sensor. *Continental Shelf Research*, *27*(6), 744–756. https://doi.org/10.1016/j.csr.2006.11.016

Philander, S. G. H. (1990). *El Niño, La Niña, and the Southern Oscillation, 293*. New York: Elsevier.

Pizarro, O., Clarke, A. J., & Van Gorder, S. (2001). El Niño sea level and current along the South American coast: Comparison of observations with theory. *Journal of Physical Oceanography*, *31*(7), 1891–1903. https://doi.org/10.1175/1520-0485(2001)031<1891:ENOSLA>2.0.CO;2

Ramage, C. S. (1975). Preliminary discussion of the meteorology of the 1972–73 El Niño. *Bulletin of the American Meteorological Society*, *56*(2), 234–242. https://doi.org/10.1175/1520-0477(1975)056<0234:PDOTMO>2.0.CO;2

Sánchez, G., Calienes, R., & Zuta, S. (1999). The 1997–1998 El Niño and its effect on the marine coastal system off Perú. *CALCOFI reports*, *41*, 62–86.

Schulz, H. N., Brinkhoff, T., Ferdelman, T. G., Hernàndez Mariné, M., Teske, A., & Jørgensen, B. B. (1999). Dense populations of a giant sulphur bacterium in Namibian shelf sediments. *Science*, *284*(5413), 493–495. https://doi.org/10.1126/science.284.5413.493

Schunck, H., Lavik, G., Desai, D. K., Großkopf, T., Kalvelage, T., Löscher, C. R., et al. (2013). Giant hydrogen sulfide plume in the oxygen minimum zone off Peru supports chemolithoautotrophy. *PLoS One*, *8*(8), e68661. https://doi.org/10.1371/journal.pone.0068661

Setoh, T., Imawaki, S., Ostrovskii, A., & Umatani, S. (1999). Interdecadal variations of ENSO signals and annual cycles revealed by wavelet analysis. *Journal of Oceanography*, *55*(3), 385–394. https://doi.org/10.1023/A:1007854415983

Thomas, A., Blanco, J., Carr, M., Strub, P., & Osses, J. (2001). Satellite-measured chlorophyll and temperature variability off northern Chile during the 1996–1998 La Niñaand El Niño. *Journal of Geophysical Research*, *106*(C1), 899–915. https://doi.org/10.1029/1999JC000052

Torrence, C., & Webster, P. (1999). Interdecadal changes in the ESNO-monsoon system. *Journal of Climate*, *12*(8), 2679–2690. https://doi.org/10.1175/1520-0442(1999)012<2679:ICITEM>2.0.CO;2

Trenberth, K. E. (1997). The definition of El Niño. *Bulletin of the American Meteorological Society*, *78*(12), 2771–2777. https://doi.org/10.1175/1520-0477(1997)078<2771:TDOENO>2.0.CO;2

Tyson, R. V., & Pearson, T. H. (1991). Modern and ancient continental shelf anoxia: An overview. In R. V. Tyson & T. H. Pearson (Eds.), *Modern and Ancient Continental Shelf Anoxia. Geological Society London Special Publications Geological Society of London*, 58, 1–24.

Weeks, S. J., Currie, B., & Bakun, A. (2002). Satellite imaging: Massive emissions of toxic gas in the Atlantic. *Nature*, *415*(6871), 493–494. https://doi.org/10.1038/415493b

Weeks, S. J., Currie, B., Bakun, A., & Peard, K. R. (2004). Hydrogen sulphide eruptions in the Atlantic Ocean off southern Africa: Implications of a new view based on SeaWiFS satellite imagery. *Deep Sea Research, Part I*, *51*(2), 153–172. https://doi.org/10.1016/j.dsr.2003.10.004

Wolter, K. (1987). The Southern Oscillation in surface circulation and climate over the tropical Atlantic, eastern Pacific, and Indian Oceans as captured by cluster analysis. *Journal of Applied Meteorology and Climatology*, *26*(4), 540–558. https://doi.org/10.1175/1520-0450(1987)026<0540:TSOISC>2.0.CO;2

Wolter, K., & Timlin, M. S. (1998). Measuring the strength of ENSO events - how does 1997/98 rank? *Weather*, *53*(9), 315–324. https://doi.org/10.1002/j.1477-8696.1998.tb06408.x